Estimating the Dynamic Stability Characteristics of Thin Shells under Follower Loads

Bulletin of Osaka Prefecture University
Series A, Vol. 45, No. 2, 1996, pp. 77-85

Estimating the Dynamic Stability Characteristics of Thin Shells under Follower Loads

Thomas GEORGE*, Nobuyoshi FUKUCHI** and Hiroo OKADA*

(Received November 29, 1996)

The stability of thin shells at large deformation states, especially of shells in the medium to deep curvature ranges, are subjected to multiple parametric influences due to the different disturbing factors present in the natural environment where they have to function as structural components. Any attempt for an accurate determination of shell stability requires elaborate theoretical and computational effort, and a detailed formulation of the shell governing equations becomes the most important task before considering any further on shell stability.

The general governing equations for thin shells are derived here in the monoclinically convected coordinates over the middle surface through tensor based formulations of continuum mechanics. Utmost care is given to the details of these derivations into their final form, where the contributions from some evidently small factors to equilibrium effects are also retained. Then, an analytical equation for the stability of the shell at different equilibrium states are derived using the method of small vibrations. Further, an analytical method is developed to determine the dynamic stability of shells by considering the disturbed small motions about the equilibrium states during large deformations.

Detailed numerical calculations were performed for the singly and doubly curved partial circular shells of shallow to deep curvature ranges. Presented here are some results on the stability characteristics and the resulting classifications for singly and doubly curved shells.

1. Introduction

Shells are used as structural components in many of the land-based and marine constructions, since they offer some specific architectural shapes, added stability and strength due to their form. The present state of knowledge of the theory of shells contains a broad spectrum of diverse approaches leading to different levels of theoretical formulations and their approximations[1-5], and numerous studies are being conducted on its advanced aspects.

This paper deals with the finite deformations and stability of shells subjected to follower loads. The governing equations for thin shells defined in a system of monoclinically convected coordinate axes derived in some of the earlier studies[6-8] are being used here, without going into the details of their derivations. All the analytic equations were derived with proper consideration of the shell geometry after deformation, which makes the results to be more exact than formulations based on the pre-deformation metric values. The systematic presentation of tensor derivations from first principles, and its physical and numerical interpretations have also been previously verified.

The results of a series of theoretical and numerical studies conducted on the subject of shell stability, especially on the stability under disturbed equilibrium conditions at the deformed states[7,8], are being summarized in this paper. Since the background material in the form of some numerical examples are being avoided in the presentation of this paper, the final results could be viewed as devoid of some supportive details. However, the essence of this paper being the qualitative summarization of the most important of the results, the self-affirmative style of presentation is assumed to be unavoidable.

Partial cylindrical and spherical shells with curvatures ranging from very shallow to very deep were considered and their stability characteristics were numerically investigated during the finite deformation process using an analytical equation developed using the method of small vibrations. The natural frequencies of vibration of the shell were monitored through the finite deformation process, which brought out the different types of instability mechanisms for each shell.

*Department of Marine System Engineering, College of Engineering
**Department of Naval Architecture and Marine Systems Engineering, Faculty of Engineering, Kyushu University

Also, numerical analyses were conducted for the dynamic stability of the shell at selected stages of its finite deformation process using another analytical equation developed by considering the disturbed small motions about the equilibrium states. This analysis has shown that there were some parametric combinations for a shell at which the dynamic instabilities occur even with the slightest amount of external disturbance.

The simply supported conditions were assumed at the shell boundaries and the Galerkin method was employed for numerical formulations. Attempts for generalizations were therefore restricted to the partial cylindrical and spherical shells with conditions as stated above. Generally, the present analytical methods and the qualitative aspects of numerical results might be extended safely to other shell types, loading and boundary conditions, some of which are under consideration presently.

2. Theoretical Formulations

The general governing equations for a thin shell are formulated here in the *monoclinically convected coordinate axes* (θ^1, θ^2, θ^3) traced over the shell middle surface, where the θ^3 direction is adopted normal to that surface, as shown in Fig. 1.

The *Kirchhoff-Love* assumptions are assumed true throughout the finite deformation process of a thin shell. The *Range Convention* adopted here for indices is such that all *Latin* indices (i, j, k,$\cdots$) take values 1, 2, 3 and *Greek* indices (α, β, γ,$\cdots$) have the range 1, 2. Various other notations and symbols used in this paper will be explained when and where they appear first.

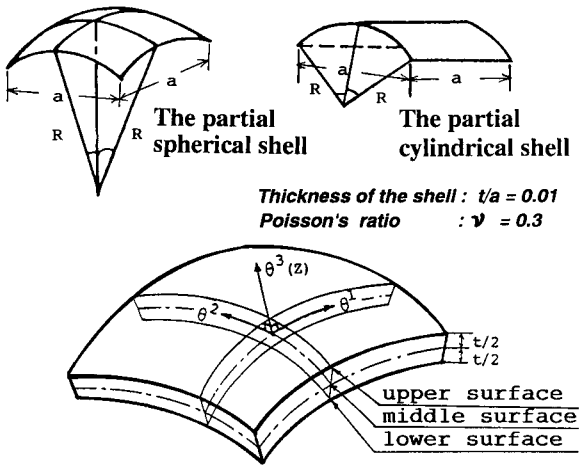

Fig.1 The definition of monoclinically convected coordinate axes and the geometry of two particular shell types

2.1 The Disturbed State of Equilibrium

The equilibrium of a shell undergoing finite deformations is prone to exhibit some unstable behavior depending on the various disturbances that accompany the state change or loading by virtue of either internal or external excitations those are present in any physical situation. The geometrical relationship between the undisturbed and disturbed states of equilibrium can be represented by the incremental variation in the position vector of any middle surface point, as shown in Fig. 2 and expressed by Eq. (1).

$$\mathbf{R}+\delta\mathbf{R}=\mathbf{r}+(\mathbf{u}+\delta\mathbf{u}) \tag{1}$$

Here, $\mathbf{r}$ and $\mathbf{R}$ are the position vectors of an undisturbed equilibrium state and $\mathbf{u}$ ($=u_i\boldsymbol{a}^i$) is the deformation vector, where $\boldsymbol{a}^i$ is the base vector of the middle surface before deformation.

This incremental property can be incorporated into the derivations of the fundamental values of a shell from the first principles of continuum mechanics. As a result, all those quantities which undergo an incremental variation may be represented both in their undisturbed and disturbed states. In the following text, a *hat* (^), a *tilde* (~) and an *asterisk* (*) signs are used over different quantities to represent the undisturbed, disturbed and the incremental change respectively.

2.2 General Governing Equations

The general surface strain of the shell is expressed using the 2-dimensional form of the *Green-Lagrange* strain tensor, and the *Cauchy* stress tensor for isotropic materials is used in its 2-dimensional form to express the stress-strain relationship on the general surface.

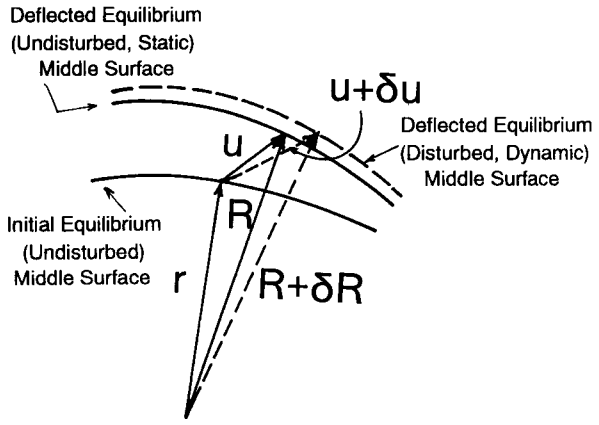

Fig.2 Position vectors and deformation vectors on the disturbed equilibrium middle surface

The membrane force tensor ($N^{\alpha\beta}$) and the moment tensor ($M^{\alpha\beta}$) may be derived through the direct integration of stress components across the shell thickness t, which is assumed to be uniform. After proper substitutions and reductions, the membrance force and the moment tensors can be expressed completely in terms of the middle surface quantities. Subsequently, the transverse shear force can be eliminated by substitutions from the equilibrium equations for the thin shell whereby, the following governing equations can be formulated for the finite deformations, which include the effects of disturbed small motions about an equilibrium state.

$$\underset{(a)}{\tilde{N}^{\alpha\beta}\|_{\alpha}}+\underset{(a)}{\tilde{M}^{\alpha\gamma}\|_{\alpha}}\tilde{B}^{\beta}_{\gamma}=-\tilde{p}^{\beta}-m^{\alpha}\tilde{B}^{\beta}_{\alpha}-\rho t\ddot{u}^{*\beta} \tag{2}$$

$$\tilde{N}^{\alpha\beta}\tilde{B}_{\alpha\beta}-\underset{(a)}{\tilde{M}^{\alpha\beta}\|_{\alpha\beta}}=-\tilde{p}^{3}+\underset{(a)}{m^{\alpha}\|_{\alpha}}-\rho t\ddot{u}^{*3} \tag{3}$$

Here, the quantity m^{α} is the sum of the surface tractions and body forces contributed moment load, p^{α} and p^{3} are respectively the tangential and normal components of applied follower load, which is uniformly distributed over the surface. B^{β}_{α} and $B_{\alpha\beta}$ denote the curvature tensors of the middle surface after deformation. The symbol ' $\|$ ' denotes 2-dimensional (*surface*) covariant differentiation with respect to the subscript that follows. Also, the symbol (a) below the covariant sign denotes differentiations performed on quantities after deformation.

The presence of inertia forces due to the disturbances are given on the righthand sides, where the double dots above the disturbance components of the deflection terms denote double differentiation with respect to the time variable τ. The resultant mass density of the shell material per unit surface area is given by ρ.

2.2.1 Representation of Stress Resultants

As stated previously, all the quantities with a *tilde* over them can be represented as the sum of their undisturbed equilibrium and disturbance components, whereby the quantities $\tilde{N}^{\alpha\beta}$ and $\tilde{M}^{\alpha\beta}$ may be expressed as follows:

$$\left.\begin{aligned}\tilde{N}^{\alpha\beta}&=\hat{N}^{\alpha\beta}+N^{*\alpha\beta}\\&=\mathrm{D}a^{\alpha\beta\delta\lambda}\tilde{\varepsilon}_{\delta\lambda}+\mathrm{K}a^{\varepsilon\beta\eta\xi}\,(b^{\phi}_{\phi}\delta^{\alpha}_{\varepsilon}\delta^{\delta}_{\eta}\delta^{\lambda}_{\xi}\\&\quad-b^{\alpha}_{\varepsilon}\delta^{\delta}_{\eta}\delta^{\lambda}_{\xi}-b^{\lambda}_{\xi}\delta^{\alpha}_{\varepsilon}\delta^{\delta}_{\eta})\tilde{\varkappa}_{\delta\lambda}\end{aligned}\right\} \tag{4}$$

$$\left.\begin{aligned}\tilde{M}^{\alpha\beta}&=\hat{M}^{\alpha\beta}+M^{*\alpha\beta}\\&=\mathrm{K}a^{\alpha\beta\delta\lambda}\tilde{\varkappa}_{\delta\lambda}+\mathrm{K}a^{\varepsilon\beta\delta\lambda}\,(b^{\phi}_{\phi}\delta^{\alpha}_{\varepsilon}-b^{\alpha}_{\varepsilon})\tilde{\varepsilon}_{\delta\lambda}\end{aligned}\right\} \tag{5}$$

$\varepsilon_{\alpha\beta}$, b^{β}_{α} and $\varkappa_{\alpha\beta}$ are respectively the strain, the initial curvature and the change of curvature tensors of the middle surface. Also, $\delta^{\alpha}_{\varepsilon}$ is the *Kronecker delta*. D and K are respectively the *extensional stiffness* and the *bending stiffness* parameters, and $a^{\alpha\beta\gamma\delta}$ is the elasticity tensor of the middle surface before deformation, as defined in the following equations.

$$\left.\begin{aligned}\mathrm{D}&=\frac{\mathrm{E}t}{(1-\nu^{2})}\\\mathrm{K}&=\frac{\mathrm{E}t^{3}}{12(1-\nu^{2})}\\a^{\alpha\beta\gamma\delta}&=\left(\frac{1-\nu}{2}\right)\left[a^{\alpha\gamma}a^{\beta\delta}+a^{\alpha\delta}a^{\beta\gamma}\right]+\nu a^{\alpha\beta}a^{\gamma\delta}\end{aligned}\right\} \tag{6}$$

Here, E is the Young's Modulus of Elasticity, ν is the Poisson's ratio and $a^{\alpha\beta}$ is the metric tensor of the middle surface before deformation.

2.2.2 Representation of Strain and Curvature

The strain tensor $\varepsilon_{\alpha\beta}$, the curvature tensor after deformation $B_{\alpha\beta}$ and the change of curvature tensor $\varkappa_{\alpha\beta}$ can be expressed through the following equations, in terms of the initial curvature tensor $b_{\alpha\beta}$ and the disturbed deflection components $\tilde{u}_{k}$ (k=1, 2, 3).

$$\left.\begin{aligned}\tilde{\varepsilon}_{\alpha\beta}&=\hat{\varepsilon}_{\alpha\beta}+\varepsilon^{*}_{\alpha\beta}\\&=\frac{1}{2}\{\tilde{u}_{\alpha,\beta}+\tilde{u}_{\beta,\alpha}-2(b_{\alpha\beta}\tilde{u}_{3}+\Gamma^{\lambda}_{\alpha\beta}\tilde{u}_{\lambda})\\&\quad+b^{\lambda}_{\alpha}b_{\lambda\beta}(\tilde{u}_{3})^{2}+\tilde{u}_{3,\alpha}\tilde{u}_{3,\beta}\\&\quad+b^{\lambda}_{\alpha}[(b^{\rho}_{\beta}\tilde{u}_{\rho}+\tilde{u}_{3,\beta})\tilde{u}_{\lambda}+(\Gamma^{\rho}_{\lambda\beta}\tilde{u}_{\rho}-\tilde{u}_{\lambda,\beta})\tilde{u}_{3}]\\&\quad+b^{\lambda}_{\beta}(\tilde{u}_{\lambda}\tilde{u}_{3,\alpha}-\tilde{u}_{\lambda,\alpha}\tilde{u}_{3})\}\end{aligned}\right\} \tag{7}$$

$$\tilde{B}_{\alpha\beta}=b_{\alpha\beta}+\tilde{\varkappa}_{\alpha\beta} \tag{8}$$

$$\left.\begin{aligned}\tilde{\varkappa}_{\alpha\beta}&=\hat{\varkappa}_{\alpha\beta}+\varkappa^{*}_{\alpha\beta}\\&=\tilde{u}_{3,\alpha\beta}-b^{\lambda}_{\alpha}b_{\beta\lambda}\tilde{u}_{3}-\Gamma^{\lambda}_{\alpha\beta}\tilde{u}_{3,\lambda}\\&\quad+(b^{\lambda}_{\beta}\tilde{u}_{3,\alpha}+b^{\lambda}_{\alpha}\tilde{u}_{3,\beta})\tilde{u}_{3,\lambda}\\&\quad+\frac{1}{2}[b^{\lambda}_{\lambda}b^{\rho}_{\rho}(\tilde{u}_{3})^{2}-b^{\lambda}_{\rho}b^{\rho}_{\lambda}(\tilde{u}_{3})^{2}]\,b_{\alpha\beta}\end{aligned}\right\} \tag{9}$$

The disturbance components $\varepsilon^{*}_{\alpha\beta}$ of the strain tensor and $\varkappa^{*}_{\alpha\beta}$ of the change of curvature tensor can be calculated directly using the method of disturbed small motions on the deflection components. The resulting expressions for these quantities can be deduced after an order evaluation into the following forms.

$$\varepsilon^*_{\alpha\beta} = -b_{\alpha\beta}u^*_3 - b^\lambda_\alpha b_{\lambda\beta}u^*_3(\hat{u}_3+\frac{1}{2}u^*_3) + \frac{1}{2}\{\hat{u}_{3,\alpha}u^*_{3,\beta}+u^*_{3,\alpha}\hat{u}_{3,\beta}+u^*_{3,\alpha}u^*_{3,\beta}\} \quad (10)$$

$$\kappa^*_{\alpha\beta} = u^*_{3,\alpha\beta} - b^\lambda_\alpha b_{\beta\lambda}u^*_3 - \Gamma^\lambda_{\alpha\beta}u^*_{3,\lambda} \quad (11)$$

2.2.3 Representation of Deflection Components

The disturbed deflection components $\tilde{u}_k$ $(k=1, 2, 3)$ can be considered here in the form of an algebraic summation series, and follows:

$$\tilde{u}_k = \sum_{i=1}^{m}\sum_{j=1}^{n}(\hat{U}_{k(i,j)} + U^*_{k(i,j)})\phi_k(\theta^1, \theta^2) \quad (12)$$

Further, the disturbed small motions alone may be considered as an exponential time dependant summation series of the deflection components.

$$u^*_k = \sum\sum U^*_k \phi_k(\theta^1, \theta^2)\exp^{i\Omega_\lambda\tau} \quad (13)$$

Here, U_k represent the deflection coefficient and $\phi_k(\theta^1, \theta^2)$ may be considered as a double trigonometric function, where θ^1 and θ^2 are the angular coordinates of the middle surface in the principal directions.

2.3 Stability of Equilibrium with Small Vibrations

The stability equations for a disturbed equilibrium state can be formulated by equating the incremental variations in the governing equations to the inertia term on the righthand sides of Eq.(2) and Eq.(3).

$$N^{*\alpha\beta}\|_{\alpha(a)} + \hat{M}^{\alpha\gamma}\|_{\alpha(a)}B^{*\beta}_\gamma + M^{*\alpha\gamma}\|_{\alpha(a)}\hat{B}^\beta_\gamma + m^\alpha B^{*\beta}_\alpha = -\rho t\ddot{u}^{*\beta} \quad (14)$$

$$\hat{N}^{\alpha\beta}B^*_{\alpha\beta} + N^{*\alpha\beta}\hat{B}_{\alpha\beta} - M^{*\alpha\beta}\|_{(a)\alpha\beta} = -\rho t\ddot{u}^{*3} \quad (15)$$

These equations can also be expressed in their partial differential forms by substituting for all the terms and making appropriate order evaluations, in the following forms.

$$Da^{\alpha\beta\gamma\delta}\{u^*_{\delta,\alpha\gamma} - u^*_{\rho,\alpha}\Gamma^\rho_{\gamma\delta} - (u^*_{\lambda,\delta}+u^*_{\delta,\lambda})\Gamma^\lambda_{\gamma\alpha} - (u^{*3}b_{\gamma\delta})_{,\alpha} + \hat{u}^3_{,\gamma}u^{*3}_{,\delta\alpha} + u^{*3}_{,\gamma}\hat{u}^3_{,\delta\alpha} + (\hat{u}^3u^{*3}b_{\rho\delta}b^\rho_\gamma)_{,\alpha}\} = -\rho t\ddot{u}^{*\beta} \quad (16)$$

$$Da^{\alpha\beta\gamma\delta}\{[u^*_{\gamma,\delta} - u^{*3}b_{\gamma\delta} + \hat{u}^3_{,\gamma}u^{*3}_{,\delta} + \hat{u}^3u^{*3}b_{\lambda\delta}b^\lambda_\gamma] (b_{\alpha\beta} + \hat{u}^3_{,\alpha\beta} - \hat{u}^3b_{\beta\rho}b^\rho_\alpha - \hat{u}^3_{,\rho}\Gamma^\rho_{\alpha\beta}) + [\hat{u}_{\gamma,\delta} - \hat{u}^3b_{\gamma\delta} + \frac{1}{2}(\hat{u}^3_{,\gamma}\hat{u}^3_{,\delta} + (\hat{u}^3)^2b_{\lambda\delta}b^\lambda_\gamma)] (u^{*3}_{,\alpha\beta} - u^{*3}b_{\beta\rho}b^\rho_\alpha - u^{*3}_{,\rho}\Gamma^\rho_{\alpha\beta})\} - Ka^{\alpha\beta\gamma\delta}u^{*3}_{,\alpha\beta\gamma\delta} = -\rho t\ddot{u}^{*3} \quad (17)$$

The disturbance components of the deflection terms given by Eq.(13) can be substituted into the above equations, which can then be expressed as an eigen value problem for the disturbed small vibrations on known values of the deflection components, as given below.

$$\mathbf{KX} = \Lambda\mathbf{X} \quad (18)$$

where, $\mathbf{X}$ denotes the modal matrix and Λ are the eigen values of the associated stability problem corresponding to a given state of disturbed equilibrium.

2.4 Stability of Equilibrium in the Normal Direction

The equation of dynamic stability for the shell can be formulated from the disturbed equilibrium equations Eq.(2) and Eq.(3). In this paper, only the stability in the normal direction is considered for the analysis, for which Eq.(3) forms the basis. Using the method of disturbed small motions, the left hand side of Eq.(3) gives the sensitivity of an equilibrium to small motions in the normal direction. The symbol S is to be used here to denote this sensitivity, as given below.

$$\mathbf{S}(\hat{u}^3, u^{*3}) = \hat{N}^{\alpha\beta}B^*_{\alpha\beta} + N^{*\alpha\beta}\hat{B}_{\alpha\beta} + N^{*\alpha\beta}B^*_{\alpha\beta} - M^{*\alpha\beta}\|_{(a)\alpha\beta} \quad (19)$$

This equation along with the corresponding inertia term given in Eq.(3), gives the equation for the dynamic stability of disturbed equilibrium states. The expanded form of the sensitivity function in terms of the metric tensor $a^{\alpha\beta}$, the strain and curvature tensors and the change of curvature tensor can be expressed as follows.

$$\begin{aligned}\mathbf{S}(\hat{u}^3, u^{*3}) = {} & \mathrm{D}\{(a^{11})^2[\hat{\varepsilon}_{11}\kappa^*_{11} + \varepsilon^*_{11}\tilde{\mathrm{B}}_{11}] \\ & + (a^{22})^2[\hat{\varepsilon}_{22}\kappa^*_{22} + \varepsilon^*_{22}\tilde{\mathrm{B}}_{22}] \\ & + a^{11}a^{22}[\nu(\hat{\varepsilon}_{11}\kappa^*_{22} + \hat{\varepsilon}_{22}\kappa^*_{11} + \varepsilon^*_{11}\tilde{\mathrm{B}}_{22} + \varepsilon^*_{22}\tilde{\mathrm{B}}_{11}) \\ & + \left(\frac{1-\nu}{2}\right)((\hat{\varepsilon}_{12}+\hat{\varepsilon}_{21})(\kappa^*_{12}+\kappa^*_{21}) \\ & + (\varepsilon^*_{12}+\varepsilon^*_{21})(\tilde{\mathrm{B}}_{12}+\tilde{\mathrm{B}}_{21}))]\} \\ & + \mathrm{K}\{(a^{11})^2[\kappa^*_{11}(\tilde{\mathrm{B}}_{11}+\hat{\kappa}_{11})(b^2_2 - b^1_1) \\ & - \kappa^*_{11,11} - \varepsilon^*_{11,11}b^2_2] \\ & + (a^{22})^2[k^*_{22}(\tilde{\mathrm{B}}_{22}+\hat{\kappa}_{22})(b^1_1 - b^2_2) \\ & - \kappa^*_{22,22} - \varepsilon^*_{22,22}b^1_1] \\ & - a^{11}a^{22}[\nu(\kappa^*_{11,22} + \kappa^*_{22,11} \\ & + \varepsilon^*_{11,22}b^1_1 + \varepsilon^*_{22,11}b^2_2) \\ & + \left(\frac{1-\nu}{2}\right)(2(\kappa^*_{12,12}+\kappa^*_{21,12}) \\ & + (\varepsilon^*_{12,12}+\varepsilon^*_{21,12})(b^1_1+b^2_2))]\}\end{aligned} \quad (20)$$

Now, the sensitivity function along with the inertia term can be combined with the parametric influences due to damping and excitation forces, giving the following final form of the parametric stability equation.

$$\ddot{u}^{*3}+\mathcal{S}(\hat{u}^3,\ u^{*3})+\mathcal{D}\dot{u}^{*3}=-\mathcal{A}\sin\Omega\tau \tag{21}$$

The notation $\mathcal{S}(\hat{u}^3,\ u^{*3})$ denotes the modified unit mass basis of the sensitivity function $\mathbf{S}(\hat{u}^3,\ u^{*3})$ defined in Eq. (20). Here, $\mathcal{D}$ is the damping coefficient and $\mathcal{A}$ is the maximum amplitude of the excitation force. The single dot above the disturbance component of the deflection term denotes differentiation with respect to the time variable τ.

Damping is arbitrarily assumed as a linear velocity function, and the excitation force is considered here as a sinusoidal function for the numerical calculations that follow. The amplitude $\mathcal{A}$ of the excitation force is interpreted here for the numerical calculations as a fraction of the static loading rate $\hat{p}^3$, using the following equation:

$$\mathcal{A}=\mathcal{P}.\ \hat{p}^3 \tag{22}$$

By virtue of this equation, the factor $\mathcal{P}$ is to be known as the *excitation amplitude factor*, and the plane formed by it with the excitation frequencies Ω defines the *excitation force field*, which forms the plane on which the numerical assessment of dynamic stability characteristics is to be made in this paper.

3. Numerical Results

The shell as a structural element requires to maintain its initial continuity and strength upto a sufficiently minimum level even at the maximum expected performance level of the total structure. The incidence of any unexpected factor, such as an external disturbance or a random excitation force, should not endanger the integrity of any element, within the normal performance ranges. Dynamic aspects, rather than statically determinable problems, may induce some instability due to the many number of unknown factors involved.

The problem of shell stability is analyzed here through different methods, first using the method of small vibrations and then by a dynamic analysis using the method of disturbed small motions. The respective analytical equations were already given in sec. 2. 3 and sec. 2. 4. Here we consider the partial cylindrical shell and the partial spherical shell as the representative types of singly curved (zero *Gaussian Curvature*) and doubly curved (positive *Gaussian Curvature*) shells. All examples given here are for shells of projected square bases of unit area and simply supported with all inplane deflections at the boundaries arrested. A uniform pressure load acting on the entire shell middle surface in the anti-radial direction is adopted. The shell thickness t is taken to be of a sufficiently small order in comparison with the radius R and the principal chord lengths $[a=l_1=l_2,\ t/a=0.01]$, to represent the fundamental assumptions properly. Curvature ranges of shells are selected from the plate $(R/a=\infty)$ to the subtended angle of π *radians* at the center $(R/a=0.5)$ for the deep shell. As a result, about 25 different curvature values each for the partial cylindrical and spherical shells are numerically analyzed here.

The differential geometry of a toroidal shell definition is used to express the basic values of the shell middle surface. The corresponding values for metric tensors, curvature tensors and other quantities can be formulated from the first principles[6]. Since the present investigation stresses on the lower modes of instability, the representation of deflection components given in Eq. (12) is truncated at the 9 th principal term $(m=3,\ n=3)$. Generally, numerical results are nondimensionalized appropriately for convenient graphical representation, as indicated thereby.

The numerical value of $E=1.96\times10^{11}\ N/m^2$ for the *Young's modulus* and the *Poisson's ratio* of $\nu=0.3$ are used for numerical calculations. Also, the material density is assumed to be $\rho=7.85\times10^3\ kg/m^3$ and the acceleration due to gravity is taken as $g=9.81\ m/s^2$. Galerkin's method and numerical integrations using the Gaussian quardrature are used for solutions of the governing equations. The QR method and the Runge-Kutta-Gill method are used for the analyses of the stability equations.

3.1 Analyses using the Method of Small Vibrations

The analytical method presented in sec. 2. 3 is used here to calculate the natural frequencies of vibration of the shell at consecutive deformed states of equilibrium. The characteristic points of different instability mechanisms are traced by studying the variation in the natural frequencies of the different modes of vibration in unison with the normal deflection curves at different points on the shell. Fig. 3 and Fig. 4 give these results in a condensed form, where the types and ranges of instability at each curvature are shown. Since the

figures are mostly self explanatory, the method of each evaluation and its justifications are not presented here for the sake of brevity.

Fig. 3 shows the case of partial spherical shells, which by virtue of the double curvatures have a complicated division of stability ranges and instability characteristics. Fig. 4 shows the case of partial cylindrical shells, which are rendered less complicated by the absence of one principal curvature, in spite of the fact that the actual evaluation of individual characteristics is eventually made more difficult for the same reason, than a doubly curved shell.

The most notable feature of these figures are the lower bounds of dynamic instability, considerably below the critical instability curves. The region of transient dynamic instability between these curves are prone to introduce instabilities of different kinds, mainly of the *mode shift* type[7], at several points of the loading history, depending on the type and amount of disturbances or other excitations.

Also, it can be noted that shells of large curvatures which are considerably 'membrane rigid' due to their deeper forms, are subject to dynamic flutters or local reverse bucklings (LRB), leading to instabilities. However, shallow shells may overcome some of the initial instabilities using their 'membrane flexibility' and are more likely to continue carrying further loads in some assumed new equilibrium state, mostly like an elastic cable. Evidently, the region of extremely shallow shells can be found to be almost completely stable, except for some transient initial instabilities which would be overcome in most cases, to continue deforming until an elastic failure occurs.

3.2 Analyses using the Method of Disturbed Small Motions

The concept of dynamic stability of a shell is quite arbitrary in the sense that the determination of an unstable behaviour depends on the allowed upper limit of dynamic state change that may be considered 'stable' at the particular load-deformation stage. The numerical analysis of the stability of thin shells under disturbed states of equilibrium are done here through

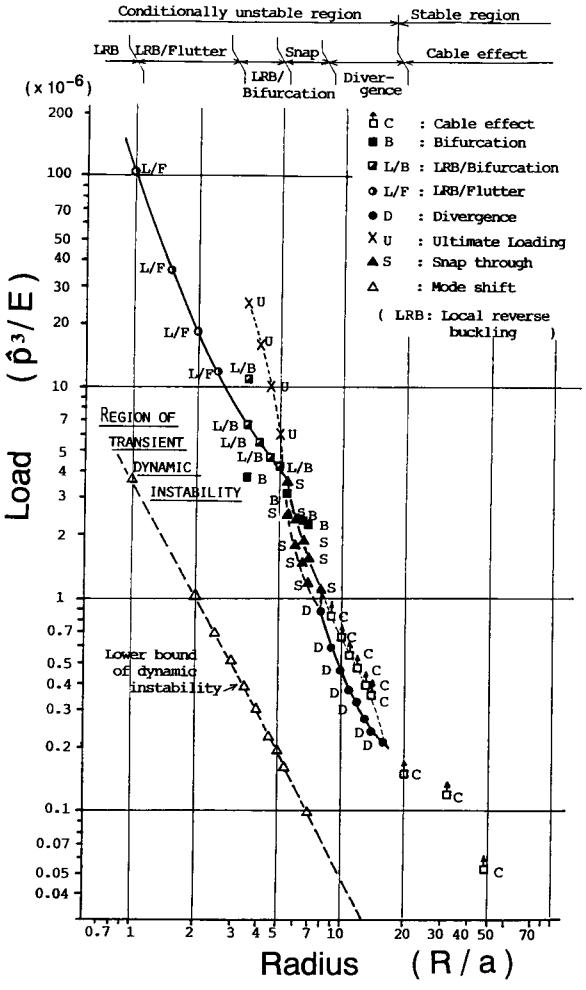

Fig.3 Stability characteristics for partial spherical shells

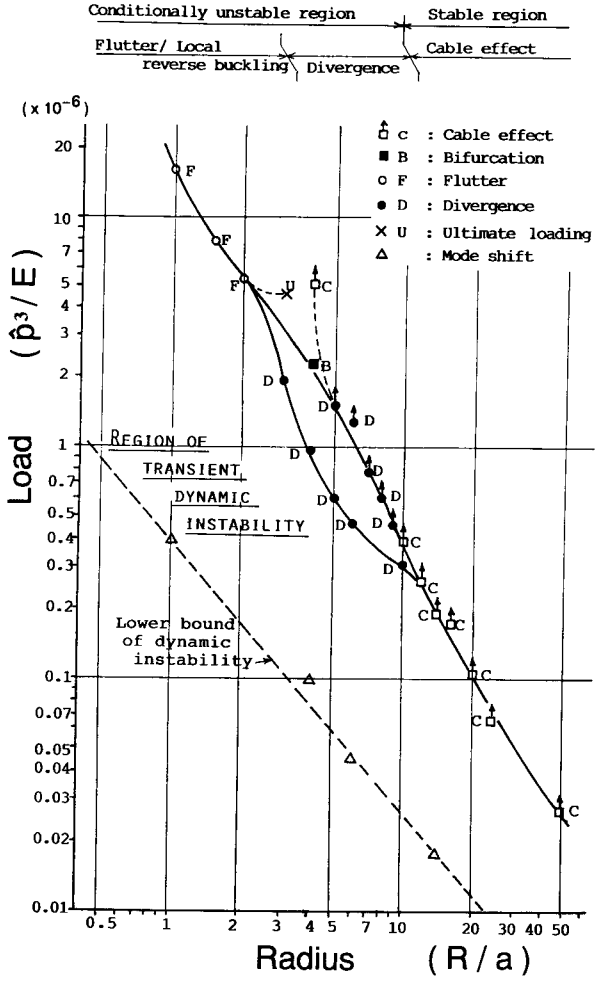

Fig.4 Stability characteristics for partial cylindrical shells

the analytic method given in sec. 2.4 using Eq. (21), where the shell is assumed to be in a virtual state of static equilibrium under a given stage of the follower load. By virtue of Eq. (21), the parametric influences of damping and excitation forces are considered here, though the damping coefficient $\mathcal{D}$ was arbitrarily assumed to be unity.

About 20 to 50 loading stages each of the 8 partial cylindrical shells and 12 partial spherical shells are analyzed here. The *mean curvatures* b_a^α, which is defined as the sum of the two *principal curvatures*, of these shells ranged between 0.05 to 3.46, since it is intended to analyze the characteristics of as wide a range of curvatures as possible.

The arbitrary assumption was made here that the $U^*_{3(I,J)}$ values start from rest at $\tau=0.0$, and their initial values are set at $(U^*_{3(I,J)}/\hat{U}_{3(I,J)})=10^{-14}$ to give a sensitivity of very high precision. The *critical stability time period* for all the *selected points for stability calculations* are truncated arbitrarily at 1.0 *sec*, provided a very conclusive stability behaviour was shown before this time period. If the *amplitude of motion of mode disturbance* $U^*_{3(I,J)}$ for all the modes remained below a specified common absolute maximum value at the end of the 'critical stability time period', then that point on the excitation force field was judged 'stable'. On the other hand, if the amplitudes diverge out and exceed the specified maximum value before the time period, then that point on the excitation force field was marked 'unstable'.

The specification for the common absolute maximum value for the amplitude of mode disturbance is fixed as the absolute maximum $\hat{U}_{3(I,J)}$ among the modes under consideration at each of the selected points for stability calculations. This value for the critical amplitude of mode disturbance was considered as the maximum allowable amount of mode disturbance within the scope of the method of disturbed small motions used for this formulation.

To provide some typical examples for the results of these analyses, the partial spherical shell of $R/a=2.0$ is selected here. Fig. 5 gives the load-deflection curves at four different points on a quarter shell along with the average deflection curve. Marked on the figure are the *selected points for stability calculations*, as P_{14}, P_{42}, P_{69}, P_{76}, P_{87}, P_{92} and P_{95} on the vertical axis, all of which fall within the region of transient dynamic instabilities. The numerical digits following each P denote

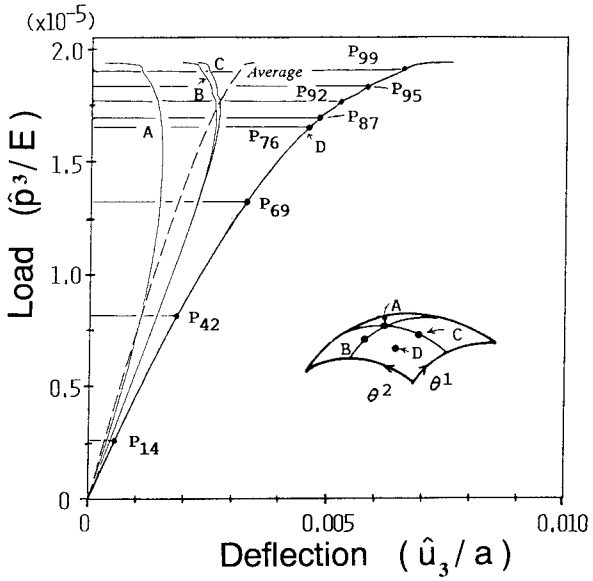

Fig.5 Deflection curves and the selected points for stability calculations (Partial spherical shell, $R/a=2.0$)

the corresponding loading stages of the equilibrium positions, approximately as a truncated percentage of the critical load $P_{cr}(=\hat{p}^3_{(critical)})$.

The load-deflection history of this shell is found to have both 'forward' and 'reverse' patterns for different points of the middle surface. Throughout this analysis the centre point of a quarter shell (point D) was selected as the monitoring point for amplitude response characteristics, for the reason that in most cases it would represent the average deflection curve most closely, and it can give both the symmetric and the unsymmetric mode histories during the stability analysis.

Fig. 6, Fig. 7 and Fig. 8 give the *excitation force field*, as defined in sec. 2.4, for the points P_{14}, P_{92} and P_{95} respectively. The lowest points of the excitation amplitude factor $\mathcal{P}$ can be seen to fall to very minute values at P_{99}. This is as a result of the impending dynamic failures at this loading stage, where even the smallest of disturbances could prove fatal to stability.

The lower bounds of such critical instability values for all the loading stages for this shell are plotted in Fig. 9. Based on the numerical evidence obtained, it can be read from this figure that the loading stage P_{92} may be treated as the stability threshold point for this shell, beyond which the loading stages become prone to dynamic instabilities even with the slightest disturbance.

In Fig. 10 the stability threshold curves for different partial spherical shells are given. From the figure, the vertical fall of the lower bounds of critical distur-

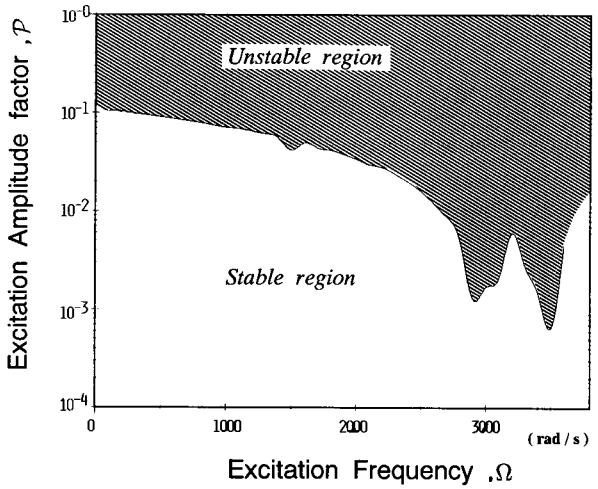

Fig.6 The excitation force field at P_{14}

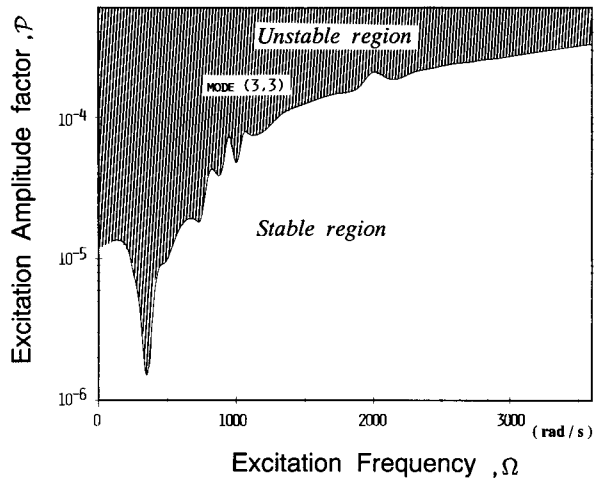

Fig.7 The excitation force field at P_{92}

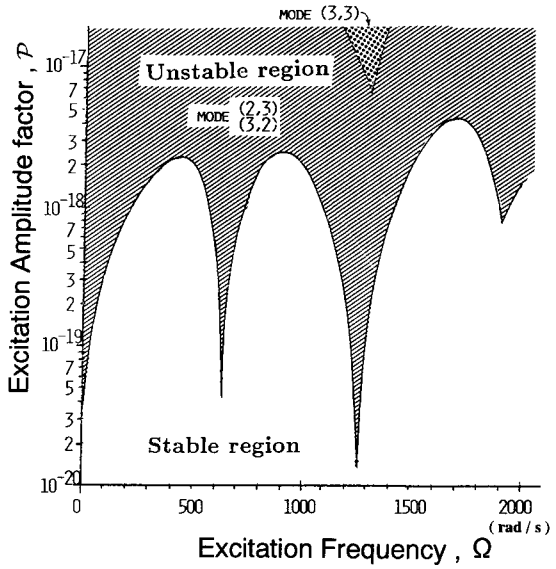

Fig.8 The excitation force field at P_{99}

bances can be seen to be a characteristic of dynamic stability threshold for each shell.

The characteristics of dynamic stability threshold

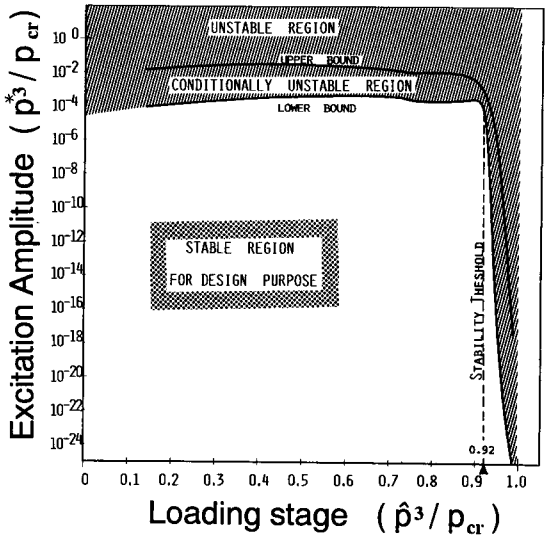

Fig.9 The dynamic stability threshold curve (Partial spherical shell, $R/a=2.0$)

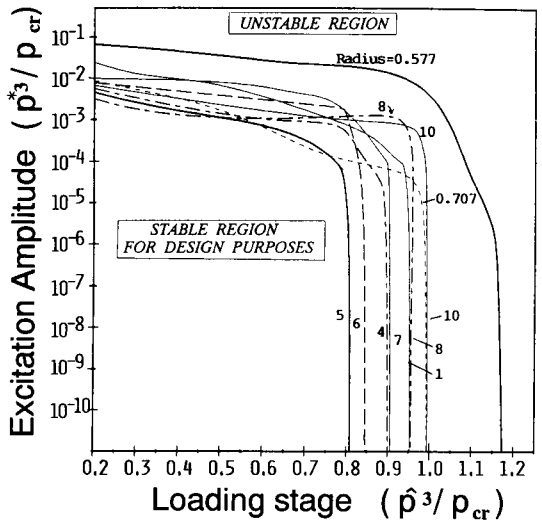

Fig.10 Dynamic stability threshold curves of partial spherical shells

for partial spherical shells are given in Fig. 11. Shallow shells can be considered as dynamically stable for all practical purposes and their design criteria for stability can be easily affixed to the static criteria alone. However, for deeper shells, especially for the medium range fo curvatures, the dynamic stability criteria has to be evaluated thoroughly and the design criteria should be based on that evaluation. A range of post-critical stability is also visible for some shells, particularly the deep shells.

Numerical results for partial cylindrical shells are not given here for the sake of brevity. An accompanying paper to this provides further explanations to possible reasons for the intricate behavior of medium deep shells through an analysis of the resisting mechanisms and strength characteristics.

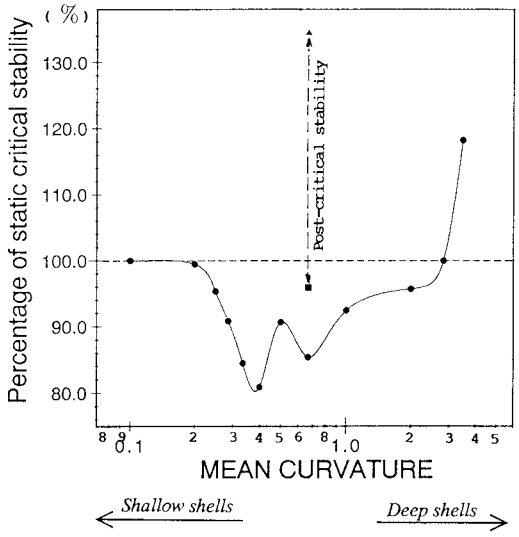

Fig.11 The Dynamic stability threshold characteristic curve of Partial spherical shells

4. Conclusions

The theoretical formulations presented here for the stability of thin shells were verified for their applicability through several numerical calculations. The stability of a shell equilibrium under disturbances could be viewed as a critical aspect depending on the loading stage. The shallow and deep ranges of curvatures were found to be mostly free from instabilities, whereas the medium range of curvatures were very prone to dynamic failures at very earlier stages of their deformation history.

Some of the disagreements found between the theory of shells and their experimental verifications might be attributed to the dynamic instabilities investigated here. Although the present numerical results were limited to some particular shell types with specific boundary and loading conditions, the qualitative aspects derived from these results would be generally applicable to other situations also.

References

1) Green, A.E., Zerna, W.: Theoretical Elasticity, Oxford University Press, Oxford (1960)
2) Bolotin, V.V.: The Dynamic Stability of Elastic Systems, Holden-Day Inc., San Francisco (1964)
3) Ziegler, H.: Principles of Structural Stability, Blaisdell Publishing Company, Massachusetts (1968)
4) Flügge, W.: Tensor Analysis and Continuum Mechanics, Springer-Verlag, New York (1972)
5) Pietraszkiewicz, W.: Geometrically Nonlinear Theories of Thin Elastic Shells, Advances in Mechanics, **12** (1989), pp. 51~130
6) Shinoda, T., George, T., Fukuchi, N.: A Detailed Analysis of the Theory of Thin Shells and some Particular Applications, Trans. of the West Japan Society of Naval Architects, No. 80 (1990), pp. 171~193
7) Fukuchi, N., George, T., Shinoda, T.: Dynamic Instability Analysis of Thin Shell Structures subjected to Follower Forces, (2 nd Report) Numerical Solutions and some Theoretical Concepts, Journal of the Society of Naval Architects of Japan, No. 171 (1992), pp. 597~609
8) George, T., Fukuchi, N.: Dynamic Instability Analysis of Thin Shell Structures subjected to Follower Forces, (6 th Report) Dynamic Threshold Characteristics and Post-critical Stability, Journal of the Society of Naval Architects of Japan, No. 176 (1994), pp. 319~330